IJRCS

International Journal of Robotics and Control Systems
Vol. 3, No. 3, 2023, pp. 396-416
ISSN 2775-2658
http://pubs2.ascee.org/index.php/ijrcs

ASCEE

Stability Analysis of Cyber-physical System Under Transmission Delay

Nezar Mohammed Al-Yazidi [a,b,1,*], Yousif Ahmed Al-Wajih [a,2], Magdi S. Mahmoud [a], Mutaz M. Hamdan [c]

[a] Department of Control and Instrumentation Engineering, King Fahd University of Petroleum and Minerals, Dhahran, Saudi Arabia
[b] Interdisciplinary Center of Smart Mobility and Logistics, King Fahd University of Petroleum and Minerals, Dhahran, Saudi Arabia
[c] Department of Mechanical Engineering, National University College of Technology, Amman 11592, Jordan,
[1] nalyazidi@kfupm.edu.sa; [2] alwajihyousif@gmail.com
* Corresponding Author

ARTICLE INFO

Article History
Received February 21, 2023
Revised May 03, 2023
Accepted June 11, 2023

Keywords
Stability analysis;
Output feedback;
Transmission delay;
Multi-areas power system

ABSTRACT

With the intimate integration of power grids and cyber networks, limited bandwidth and packet delay have a rapidly expanding negative impact on power system performance. The presented multi-area interconnected power system consists of four areas, each including thermal and hydro-generation plants. This paper investigates the stability analysis problem for cyber-physical systems with a round-robin communication protocol under mixed cyberattacks and load changes. The objective is to stabilize a multi-area interconnected power system (MAIPS) using a static feedback controller while minimizing the defined performance function. Then, the stability of the MAIPS is characterized when the system is subjected to a transmission delay while considering predetermined limits for the duration and the frequency of the delay. Our findings indicate that time delays can influence system stability and that choosing an appropriate sampling interval is necessary to ensure the stability of the system. Finally, an illustrative example of three areas of interconnected power systems with several scenarios is presented to verify the effectiveness of the proposed method.

1. Introduction

Recent advances in power systems have increased attention to the multi-area interconnected power system (MAIPS). To support control schematics in power systems, recent research has focused on applying different virtual inertia emulation methods to link the multi-power generations [1, 2, 3, 4]. The control loops of load frequency control (LFC) send measurements and control data among networks such as the supervisory control and data acquisition (SCADA) system. Load frequency control is a crucial aspect of maintaining the stability of a power system. In power systems, the demand for electricity fluctuates constantly, and the supply must be adjusted accordingly to maintain a constant frequency. LFC is responsible for ensuring that the power supply matches the demand by adjusting the output of the generators in real time.

The standard control scheme of the LFC requires additional modifications to handle the new

scenarios where power generation areas are interconnected. Transmission delay, which is the time it takes for signals to travel through the power grid, can significantly impact the effectiveness of LFC. Delayed signals can cause a mismatch between supply and demand, leading to instability and even blackouts. Therefore, reducing transmission delay is essential for maintaining a stable power system and ensuring a reliable electricity supply to consumers. Therefore, high dependence on data communication introduces time delay issues in the LFC since an interconnected power system, in this manner has a high possibility of being affected by a transmission delay that has the same effect as the denial-of-service attack [5, 6]. In addition, intentionally delaying the transmission of signals through the LFC system can have a direct impact on the stability and frequency of the system. It could also lead to significant damage to the economy of the interconnected power system. In such a scenario, the transmission delay could disrupt the practical operation of the interconnected system, thereby affecting its dynamics [7]. Therefore, it is important to consider stability analysis when designing a MAIPS [8]. Therefore, it is important to consider stability analysis when designing a MAIPS [9].

Cyberattacks targeting power systems represent a significant threat to the security and stability of the electricity grid. The integration of cyber devices into power systems, such as intelligent electronic devices and information communication technology devices, has led to a high number of software vulnerabilities that malicious actors can exploit to cause severe physical consequences within power systems. For example, attackers may manipulate the supervisory control and data acquisition (SCADA) system in a substation to launch false data injection, replay, or denial-of-service attacks. These attacks can disrupt the regular operation of power systems and cause cascading failures, equipment damage, or blackouts [10].

Load frequency control (LFC) is an automatic closed-loop system that maintains the stability of the interconnected system's frequency in multi-area integrated power systems. This is achieved by adjusting the set-points of area generators for active power output based on reserved measurement through communication networks and wide-area transmitted measurement units [11]. However, LFC systems are vulnerable to cyberattacks as communication channels in wide-area measurements such as SCADA systems can be affected by attackers. Therefore, it is important to pay more attention to the security of LFC systems against cyberattacks [12].

In multi-area integrated power systems (MAIPS), communication between generation areas occurs over a common network medium. This network must be protected against attacks during data transmission. Failure to do so could result in system volatility or redundancy in plant operation. Therefore, it is essential to consider security issues when designing controllers for the MAIPS [13, 14]. Transmission delay refers to the time lag between the generation and consumption of electrical energy and can have a significant impact on the stability of power systems. This delay may arise due to physical distance, communication latency, or network congestion, among other factors. The occurrence of transmission delays in power systems can give rise to errors and uncertainties in state estimation, control, and protection. Such inaccuracies and delayed synchrophasor measurements have the potential to impact the performance and coordination of distributed controllers, including generators, inverters, and load-shedding devices. In practical applications, transmission delay can cause a critical failure of the system's performance, particularly in networked control systems like MAIPSs, where time delays during transmission can destabilize the closed-loop system and degrade its dynamics performance [13], [15].

The effect of transmission delay on conventional LFC systems with AC transmission lines has been a topic of interest in recent research. However, only a few studies have examined the impact of transmission delay on power network systems [16], [17]. A micro-grid LFC system with constant communication delays was proposed in [18], where delay margins for PI gains were derived. A decentralized LFC strategy based on switching control theory with transmission delay in the subsystem was presented in [9, 19], while a load frequency control problem with constant and time-varying

delays in state and control input was investigated in [17].

The small gain approach has been widely used by researchers to solve the stabilization problem of distributed systems. In order to maintain the stability of large-scale systems with a limited communication medium, an event-triggered sampling scheme with distributed controllers was investigated in [20]. Moreover, Song et al. proposed a robust pinning synchronization control method to ensure the recovery of the initial state for a complex system under mixed attacks in independent transmission channels [21]. A hierarchical game technique was introduced in [22] to address the control challenge of a wirelessly networked control system subject to a DoS attack.

The subject under consideration entails the design of an output feedback controller and a parameter-based method that ensures stability of a Multi-Area Integrated Power System (MAIPS) subject to load deviation and transmission delay. The present study offers the following contributions:

- Firstly, an output feedback controller is proposed to stabilize a multi-area integrated power system in the presence of load deviations and denial of service (DoS) attacks.
- Secondly, this research puts forth a load frequency control (LFC) technique for the power system that incorporates the networking infrastructure features of the sample period and packet delay. A stability condition for a particular control system is established using Lyapunov theory. The stability criterion specifies the sample period and packet delay bands that ensure the power system's stability under the supplied control.
- Thirdly, the stability of a discrete-time MAIPS is discussed and analyzed such that stability is maintained even in the presence of transmission delay and load changes.
- Fourthly, this paper characterizes the limits on the frequency and duration of transmission delay for a MAIPS that implements a typical round-robin communication protocol.
- Lastly, an illustrative example of a typical MAIPS is provided with several scenarios that consider the designed controller with typical and modified sampling intervals, both in the absence and presence of transmission delay. These scenarios are utilized to verify the effectiveness of the proposed approach and controller.

The rest of this paper is organized as follows: Section 2 presents the modeling of a MAIPS. In Section 3, we provide the framework. Then, in Section 4, we discuss the output feedback controller and stability analysis of a MAIPS. In Section 5, we present a simulation of an illustrative example. Finally, in Section 6, we conclude our work.

Table 1. Generation areas parameters [23]

Symbol	Definition
ω	Angular rotating mass frequency
M_i^a	Angular momentum of $i-th$ subsystem
P_{mech}	Mechanical power
P_v	Steam valve position
T_{ch}	Prime mover charging time constant
f_i	Non-frequency-sensitive load change deviation
R^f	Percent Change in frequency divided by percent change in unit output
D_i	Change in percentage of (load/change in frequency)
T_g	Time constant of governor
T_{ij}	Slope of the power angle curve at the initial operating angle between area i and area j
T_{tie}^{ij}	Power flow of the tie-line between area i and area j
$T_{tie,i}$	Total power flow of the tie-line between area i and area j

2. Multi-area Interconnected Power System Model

This brief considers a discrete-time MAIPS model that is linearized around operation points. The MAIPS of thermal power stations with single-state turbines equipped with PI controllers is used. The mathematical model of the time-invariant MAIPS is represented in this brief (1).

Let N denote a set of indexed areas that are connected through tie-lines. In this case, subsystems are connected through a communication network, and the model that describes this is as follows:

$$\begin{aligned} x_i(k+1) &= A_{ii}x_i(k) + B_iu_i(k) + E_if_i(k) + \sum_{j\in N} A_{ij}x_j(k) \\ y_i(k) &= C_ix_i(k) \end{aligned} \tag{1}$$

In this brief, $x_i(k) = [\Delta\omega, \Delta P_{mech}, \Delta P_{vi}, \Delta P_{tie,i}]^T \in \Re^n$ represents the states of the system's frequency deviation, mechanical power deviation, steam valve position deviation, and deviation of the total tie-line power flow. $u_i \in \Re^m$ denotes the control signal of each subsystem, while $y_i \in \Re^p$ denotes the system observation. N refers to the set of connected subsystems, and f_i represents the local variation on the demeaned load. In [23] the model is discussed in detail. The system matrices are defined as follows:

$$\begin{aligned} A_{ii}(N_{ij}) &= \begin{bmatrix} -\frac{D_i}{M_i^a} & \frac{1}{M_i^a} & 0 & -\frac{1}{M_i^a} \\ 0 & -\frac{1}{T_{CH_i}} & \frac{1}{T_{CH_i}} & \\ -\frac{1}{R_i^f T_{gi}} & 0 & -\frac{1}{T_{gi}} & 0 \\ \sum_{j\in N} T_{ij} & 0 & 0 & 0 \end{bmatrix} \\ B_i &= \begin{bmatrix} 0 \\ 0 \\ 0 \\ \frac{1}{T_{g_i}} \end{bmatrix}, \qquad E_i = \begin{bmatrix} -\frac{1}{M_i^a} \\ 0 \\ 0 \\ 0 \end{bmatrix} \\ A_{ij} &= \begin{bmatrix} 0 & 0 & 0 & 0 \\ 0 & 0 & 0 & 0 \\ 0 & 0 & 0 & 0 \\ \sum_{j\in N} T_{ij} & 0 & 0 & 0 \end{bmatrix} \\ C_i &= [1 \quad 0 \quad 0 \quad 1] \end{aligned}$$

Table 1 of generation area parameters for multi-area integrated power systems includes various parameters related to generators located in different regions. These parameters are mechanical power, power flow, angular rotating mass frequency, governor time constant, and frequency or load change. They are essential for maintaining the power system's stability and reliability. Mechanical power is the rate of energy production and conversion to electrical power by the generator. Power flow is the amount of electrical power transferred between the areas. The angular rotating mass frequency is the speed of the generator's rotor rotation. The governor time constant is the speed of the governor's reaction to a load variation. The frequency or load change is the system's reaction to changes in power demand. These parameters are applied in various power systems analysis methods, such as transient stability analysis and frequency response analysis, to ensure that the power system operates safely and can cope with disturbances. Considering the MAIPS described by the model (1). The target is to design a control system to guarantee the closed-loop stability of all areas on the power network. N in the model is representing the set of the neighbor's agent j. In this manner, the controller proposes to use the output feedback measurements of the subsystems to compute the input control signals for each time step as a distributed system. The controller's goal is to ensure the stability of the MAIPS. The diagram of the system with three areas was shown in Fig. 1.

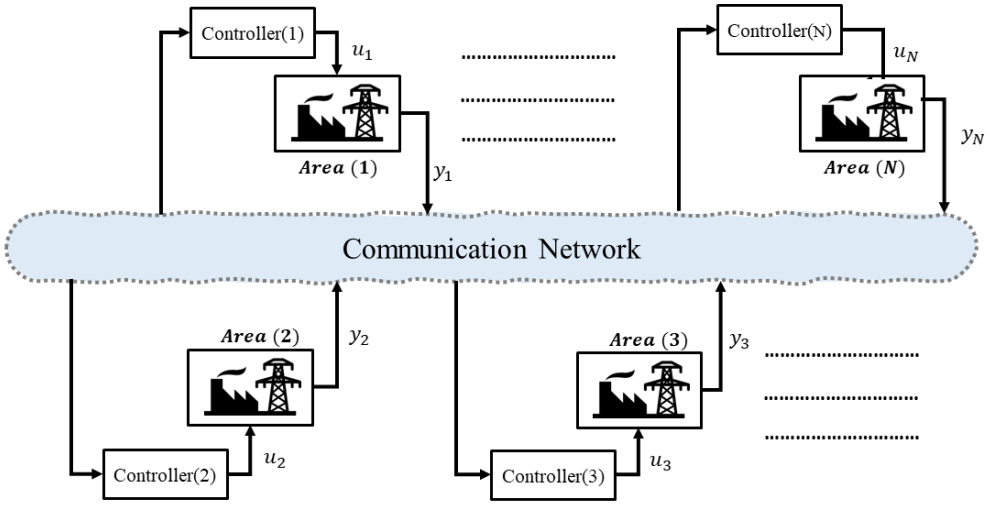

Fig. 1. Scheme of Multi-area Interconnected Power System

3. Framework

Let's consider the discrete MAIPS expressed in Section 2. In (1), we find the mathematical model of the $i-th$ subsystem on MAIPS. A wireless communication network is used to transfer data and measurements. A feedback controller uses these measurements to determine control signals and forward them to the systems' actuators to maintain a certain frequency of the grid at the desired frequency. In an ideal situation, signals arrive at the control unit with no time delay in a sample-and-hold manner. For example, $y_i(k_i^r)$ where k_i^r refers to received communication attempts.

Remark 1 *We assume that output feedback gains K_i and L_{ij} exist that press all eigenvalues of matrix A_{ii} to have a norm strictly less than one. In other words, each feedback area is Schur stable.*

3.1. Transmission Delay

In this section, we introduce a time delay in the multi-area interconnected power system. To represent this time delay on the MAIPS, we consider the sampling time T_s with a constant sampling period $T_s = t_{k+1} - t_k$ and a stochastic time delay d_k. We rewrite the sampling period at the controller as in Assumption 1.

Assumption 1 *Let h be the fixed ideal period of sampling and the delay d_k be random and limited to $d_k < d_{max}$.*

$$T_s = h + d_k \tag{2}$$

where d_k and h_k are restricted to this condition $0 < d_k < h_k$ and $0 < h_{min} < h_k < h_{max}$. However, d_k is independent and has a known distribution with an occurring frequency f_k.

Assumption 2 *Let the constants $\lambda \in \mathbb{N}, \theta \in \mathbb{N}$ and d_{max} and f_{max} exist such that time delay $d_k \in [\tau, k]$ and f_{max} have the following constraints :*

$$\begin{aligned} \mid d_k \mid &\leq \lambda + d_{max}(k-\tau) && (3) \\ f_d &\leq \theta + \frac{(k-\tau)}{f_{max}} && (4) \end{aligned}$$

Where $k \geq \tau$ for all k and τ.

We remark that the communication network generated a time delay d_k that is less than h_k but the packets were correctly received. By considering discrete-time dynamic (1) with measurements delay d_k. The subsystem dynamic is written as:

$$y_i^d(k) = \begin{cases} C_i x_i(k-d_k) & ,\gamma(k)=1 \\ C_i x_i(k) & ,\gamma(k)=0 \end{cases} \quad (5)$$

Where $\gamma(k)$ is a Bernoulli random variable with $P_r(k=1)=p_k$. y_i^d refer to received measurements of $i-th$ area.

Remark 2 *Each control input u_i affecting subsystem i consists of two parts. The first part depends on the area output with a gain of K_i, the second one depends on the area neighbors' output with a gain of L_{ij}, such control signal is given by:*

$$u_i(k) = K_i y_i^d(k) + \sum_{j \in N_i} L_{ij} y_i^d(k) \quad (6)$$

Where K_i and L_{ij} denote the controller gains.

4. Output Feedback Controller and Stability Analysis

The aim is to administrate the stability of the MAIPS in the normal situation or with the presence of the communication time delay. Mainly we address the stabilization problem of MAIPS connected by tie-line in the nominal situation and under the influence of transmission delay.

At each transmission instant, let $e_i(k)$ refer to the error between the received states $x_i^d(k)$ and the actual states $x_i(k)$ in each i-area. So, it could be written as:

$$e_i(k) = x_i^d(k) - x_i(k), \quad i = 1, 2, \ldots, N \quad (7)$$

The objective of this work is to design an output feedback controller as in (6) that guarantee the stability of the close loop model described in (1). On the coming section, the Lyapunov theory is used to ensure the system (1) is exponentially stable.

The $i-th$ subsystem dynamic could be rewritten by substituting (7) and (6) in (1), such as

$$\begin{aligned} x_i(k+1) &= A_{ii}^c x_i(k) + B_i K_i C_i e_i(k) + E_i f_i(k) + \sum_{j \in N} A_{ij}^c x_j(k) + \sum_{j \in N} B_i L_{ij} C_j e_j(k) \quad (8) \\ A_{ii}^c &= A_{ii} + B_i K_i C_i, \quad A_{ij}^c = A_{ij} + B_i L_{ij} C_j \end{aligned}$$

From close loop system (8), It could be noted that $i-th$ area is effected by the $f_i(k)$ in additional to $x_j(k)$, $e_i(k)$, and $e_j(k)$ the interconnected neighbors and errors, respectively.

Remark 3 *As illustrated in (8) stability can be achieved in a weak couplings situation and within a small error $e_i(k)$. Besides, a design parameter σ has been introduced to clarify the "smallness" of $e_i(k)$.*

Assumption 3 *(Inter-sampling interval). With nonexistence transmission delay there is an inter-sampling interval (Δ) satisfying:*

$$\|e_i(k)\| \leq \sigma_i \|x_i(k)\| \tag{9}$$

σ_i here is holds as a design factor. According to [24], the selection and design of Δ and σ_i is essential to guarantee the stability of the distributed systems.

Remark 4 *Even if Δ is not shown explicitly in (9), it can be noticed from the definition of the error (7) that the inter-sampling interval affects the stability of the system. Referring to Remark 3, Assumption 3 guarantees the "smallness" of the error by selecting a proper inter-sampling interval.*

Remark 5 *It is worth mentioning that designing the inter-sampling interval, Δ in (9) is a considerable problem. An inter-sampling interval satisfying limits as (9) could be precisely resolved for centralized settings [24]. While some literature computes and applies a lower bound of time elapsed between two events to avoid Zeno behavior in asymptotically stable distributed/decentralized systems [25], [26].*

4.1. Static Output Feedback Control Design

In this section, the main objective is to design a static output feedback controller in the form of (6) to achieve the asymptotic stability for nominal distributed systems (1). For static output feedback control design, the following two theorems are established.

Theorem 1 *If the controller gains K_i and L_{ij} in (6) is given. The system in (1) is asymptotically stable if positive matrices P_i exist and satisfy the following:*

$$\Xi_i = \begin{bmatrix} \Xi_{1i} & \Xi_{2i} & \Xi_{3i} & \Xi_{4i} & \Xi_{5i} \\ * & \Xi_{6i} & \Xi_{7i} & \Xi_{8i} & \Xi_{9i} \\ * & * & \Xi_{10i} & \Xi_{11i} & \Xi_{12i} \\ * & * & * & \Xi_{13i} & \Xi_{14i} \\ * & * & * & * & \Xi_{15i} \end{bmatrix} < 0 \tag{10}$$

Where

$$\begin{aligned}
\Xi_{1i} &= A_{ii}^{cT} P_i A_{ii}^{cT} - P_i, \quad \Xi_{2i} = 2A_{ii}^{cT} P_i B_i K_i C_i; \\
\Xi_{3i} &= 2A_{ii}^{cT} P_i E_i, \quad \Xi_{4i} = 2A_{ii}^{cT} P_i \sum_{j \in N} A_{ij}^{c}, \\
\Xi_{5i} &= 2A_{ii}^{cT} P_i \sum_{j \in N} B_i L_{ij} C_j, \quad \Xi_{6i} = C_i^T K_i^T B_i^T P_i B_i K_i C_i, \\
\Xi_{7i} &= 2C_i^T K_i^T B_i^T P_i E_i, \quad \Xi_{8i} = 2C_i^T K_i^T B_i^T P_i \sum_{j \in N} A_{ij}^{c}, \\
\Xi_{9i} &= 2C_i^T K_i^T B_i^T P_i \sum_{j \in N} B_i L_{ij} C_j, \quad \Xi_{10i} = E_i^T P_i E_i \\
\Xi_{11i} &= E_i^T P_i \sum_{j \in N} A_{ij}^{c}, \quad \Xi_{12i} = E_i^T P_i \sum_{j \in N} B_i L_{ij} C_j \\
\Xi_{13i} &= \sum_{j \in N} A_{ij}^{cT} P_i A_{ij} A_{ij}^{c}, \quad \Xi_{14i} = \sum_{j \in N} A_{ij}^{cT} P_i B_i L_{ij} C_i \\
\Xi_{15i} &= \sum_{j \in N} C_j^T L_{ij}^T B_i^T P_i B_i L_{ij} C_j
\end{aligned} \tag{11}$$

Proof 1 *To proof Theorem 1, the following Lyapunov function is considered.*

$$V_i(k) = x_i^T(k) P_i x_i(k) \tag{12}$$

By manipulating $\Delta V_i(k))$ using (11) we obtain:

$$\begin{aligned}
\Delta V_i(k) &= V_i(k+1) - V_i(k) \\
&= x_i^T(k)(\Xi_{1i})x_i(k) + 2x_i^T(k)\Xi_{2i}e_i(k) \\
&\quad +2x_i^T(k)\Xi_{3i}f_i(k) + 2x_i^T(k)\Xi_{4i}x_j(k) \\
&\quad +2x_i^T(k)\Xi_{5i}e_j(k) + e_i^T(k)\Xi_{6i}e_i(k) \\
&\quad +2e_i^T(k)\Xi_{7i}f_i(k) + 2e_i^T(k)\Xi_{8i}x_j(k) \\
&\quad +2e_i^T(k)\Xi_{9i}e_j(k) + f_i^T(k)\Xi_{10i}f_i(k) \\
&\quad +2f_i^T(k)\Xi_{11i}x_j(k) + 2f_i^T(k)\Xi_{12i}e_j(k) \\
&\quad + \sum_{j\in N} x_j^T(k)\Xi_{13i}x_j(k) + 2\sum_{j\in N} x_j^T(k)\Xi_{14i}e_j(k) \\
&\quad + \sum_{j\in N} e_j^T(k)\Xi_{14i}e_j(k)
\end{aligned} \tag{13}$$

Now, let

$$\Theta_i^T(k) = \begin{bmatrix} x_i(k) & e_i(k) & f_i(k) & \sum_{j\in N} x_j(k) & \sum_{j\in N} e_j(k) \end{bmatrix}^T \tag{14}$$

The aforementioned expression (13) is rewritten in a compact form using (14) as :

$$\Delta V_i(k) = \Theta_i^T(k)\Xi_i\Theta_i(k) \tag{15}$$

The main result is summarized by the following theorem:

Theorem 2 *If there exist positive definite matrices X_i, Y_i, Y_{ij}, M_i, R_i, M_{ij}, R_{ij}, and positive scalars ϵ_i such that the following bilinear matrix inequality (BMI) is satisfied*

$$\bar{\Xi}_i = \begin{bmatrix} -X_i & 0 & 0 & 0 & 0 & Y_i^T B_i^T + X_i A_{ii}^T \\ 0 & -\epsilon_i I & 0 & 0 & 0 & Y_i^T B_i^T \\ 0 & 0 & -\epsilon_i I & 0 & 0 & X_i E_i^T \\ 0 & 0 & 0 & -\epsilon_i I & 0 & \sum_{j\in N} Y_j^T B_i^T + X_i A_{ij}^T \\ 0 & 0 & 0 & 0 & -\epsilon_i I & \sum_{j\in N} Y_j^T B_i^T \\ * & * & * & * & * & -X_i \end{bmatrix} < 0$$
$$M_i C_i = C_i X_i, \qquad M_{ij} C_j = C_j X_i \tag{16}$$

Then, the system (8) is asymptotic stable with the designed observer controller in (6) where K_i, and L_{ij} are given as:

$$K_i = R_i M_i^{-1}, \quad L_{ij} = R_{ij} M_{ij}^{-1} \tag{17}$$

Proof 2 *Ξ_i in LMI (10) can be rewritten as:*

$$\Xi_i = \bar{\Xi}_{i11} + \bar{\Xi}_{i12} P_i \bar{\Xi}_{i12}^T < 0 \tag{18}$$

with $\bar{\Xi}_{i11} = diag\{-P_i, 0, 0, 0, 0\}$ and $\bar{\Xi}_{i12}^T = \begin{bmatrix} A_{ii}^c & B_i K_i C_i & E_i & \sum_{j\in N} A_{ij}^c & \sum_{j\in N} B_i L_{ij} C_j \end{bmatrix}^T$. So, (18) is formulated using Schur complements as:

$$\begin{bmatrix} \bar{\Xi}_{i11} & \bar{\Xi}_{i12} \\ \bar{\Xi}_{i12}^T & -P_i^{-1} \end{bmatrix} < 0 \tag{19}$$

Now, let $X_i = P_i^{-1}$, and multiply (19) from left and right by diag$\{X_i, X_i, X_i, X_i, X_i, I\}$. Recalling of the values of A_{ii}^c, and A_{ij}^c and selecting $M_i\bar{C}_i := \bar{C}_i X_i$, $R_i := K_i M_i$, $Y_i := R_i C_i$, $M_{ij}C_j := C_j X_i$, $R_{ij} := L_{ij}M_{ij}$, and $Y_{ij} := R_{ij}C_j$, the BMI can be obtained as in (16).

Remark 6 *Theorem 2 was established in view of the work presented by Mahmoud and Nounou in [27].*

4.2. A Small-Gain Approach for a MAIPS

By choosing the Lyapunov function $V_i(k) = x_i^T(k)P_i x_i(k)$ where $Q_i = Q_i^T > 0$, and P_i is the unique solution of the Lyapunov equation $\bar{A}_i^T P_i A_{ii} - P_i + Q_i = 0$. Then each subsystem i should satisfy:

$$\lambda_{\min}(P_i)\|x_i(k)\|^2 \leq V_i(x_i(k)) \leq \lambda_{\max}(P_i)\|x_i(k)\|^2 \tag{20}$$

thus $\lambda_{\min}(P_i)$ is the smallest eigenvalue of of P_i and $\lambda_{\max}(P_i)$ is the largest. To maintain the stability of the system, σ_i must be selected based on the Lemma 1.

Lemma 1 *For MAIPS described by (1) that controlled by (6). Let $\mu \in \mathbb{R}_+^N$ to be any column vector satisfy $\mu^T A < 0$. Then, the MAIPS is asymptotically stable if there is $\sigma_i \forall i \in N$ such that*

$$\sigma_i < \sqrt{\frac{l_i}{j_i}} \tag{21}$$

Where for l_i refers to the i-th vector of $L := \mu^T(-A+\bar{\Psi})$and j_i refers to the j-th vector $J := \mu^T\Gamma$. The matrices A, Γ and Ψ are defined below.

Proof 3 *Evaluating the Lyapunov function difference (13) based on (12), taking the norm and utilizing Young's inequalities lead us to*

$$\begin{aligned}
\Delta V_i(k) \quad \leq \quad & -\lambda(Q_i)\|x_i(k)\|^2 + \|\Xi_{1i}\|\left\|x_i^T(k)\right\|\|e_i(k)\| \\
& + \|\Xi_{5i}\|\left\|x_i^T(k)\right\|\|e_i(k)\| + \|\Xi_{3i}\|\left\|x_i^T(k)\right\|\|f_i\| \\
& + \|\Xi_{4i}\|\left\|x_i^T(k)\right\|\|x_j(k)\| + \|\Xi_{6i}\|\|e_i(k)\|^2 \\
& + \|\Xi_{9i}\|\left\|e_i^T(k)\right\|\|e_i(k)\| + \|\Xi_{7i}\|\left\|e_i^T(k)\right\|\|f_i\| \\
& + \|\Xi_{8i}\|\left\|e_i^T(k)\right\|\|x_j(k)\| + \|\Xi_{15i}\|\left\|e_j^T\right\|\|e_j(k)\| \\
& + \|\Xi_{12i}\|\|f_i\|^2 + \|\Xi_{14i}\|\left\|e_j^T(k)\right\|\|x_j(k)\| \\
& + \|\Xi_{10i}\|\|f_i\|^2 + \|\Xi_{11i}\|\left\|f_i{}^T\right\|\|x_j(k)\| + \|\Xi_{13i}\|\|x_j(k)\|^2
\end{aligned} \tag{22}$$

By rewriting the inequalities (22) in matrix form:

$$\begin{aligned}
\Delta V_i(x_i(k)) \leq & -\alpha_{ii}\|x_i(k)\|^2 + \psi\|f_i\| + \sum_{j\in N_i}\alpha_{ij}\|x_j(k)\|^2 \\
& + \gamma_{ii}\|e_i(k)\|^2 + \sum_{j\in N_i}\gamma_{ij}\|e_j(k)\|^2
\end{aligned} \tag{23}$$

Where α_i, α_{ij}, γ_{ii}, γ_{ij}, and ψ_i are written as

$$A = \begin{bmatrix} -\alpha_{11} & \alpha_{12} & \cdots & \alpha_{1N} \\ \alpha_{21} & -\alpha_{22} & \alpha_{23} & \alpha_{2N} \\ \vdots & \vdots & -\alpha_{33} & \vdots \\ \alpha_{N1} & \alpha_{N2} & \cdots & -\alpha_{NN} \end{bmatrix} \tag{24}$$

$$\Gamma = \begin{bmatrix} \gamma_{11} & \gamma_{12} & \cdots & \gamma_{1N} \\ \gamma_{21} & \gamma_{22} & \gamma_{23} & \gamma_{2N} \\ \vdots & \vdots & \vdots & \vdots \\ \gamma_{N1} & \gamma_{N2} & \cdots & \gamma_{NN} \end{bmatrix}$$

$$\Psi = \begin{bmatrix} \psi_{11} & & \\ & \ddots & \\ & & \psi_{NN} \end{bmatrix} \tag{25}$$

(26)

with

$$\alpha_{ii} = \lambda_{\min}(Q_i) - \delta - \sum_{j \in N_i} 2\delta + \frac{1}{\delta} \left\| 2A_{ii}^{cT} P_i E_i \right\|^2 \tag{27}$$

$$\begin{aligned} \alpha_{ij} = {} & \frac{1}{\delta} \left\| 2A_{ii}^{cT} P_i A_{ij} \right\|^2 \\ & + \frac{1}{\delta} \left\| 2 + \frac{1}{\delta} \left\| 2K_i^T C_i^T B_i^T P_i A_{ii} \right\|^2 C_i^T L_{ij}^T B_i^T P_i A_{ij} \right\|^2 \\ & + \left\| A_{ij}^{cT} P_i A_{ij} \right\|^2 \end{aligned} \tag{28}$$

$$\begin{aligned} \gamma_{ii} = {} & \frac{1}{\delta} \left\| 2A_{ii}^{cT} P_i B_i K_i C_i \right\|^2 \\ & + \sum_{j \in N} \frac{1}{\delta} \left\| 2A_{ii}^{cT} P_i B_i L_{ij} C_j \right\|^2 \\ & + \left\| C_i^T K_i^T P_i B_i K_i C_i \right\| + \sum_{j \in N} 3\delta \end{aligned} \tag{29}$$

$$\begin{aligned} \gamma_{ij} = {} & \frac{1}{\delta} \left\| 2C_i^T K_i^T B_i^T P_i B_i L_{ij} C_j \right\|^2 \\ & + \frac{1}{\delta} \left\| 2C_j^T L_{ij}^T B_i^T P_i B_i L_{ij} C_j \right\|^2 \\ & + \frac{1}{\delta} \left\| 2C_i^T L_{ij}^T B_i^T P_i E_i \right\|^2 \end{aligned}$$

$$\psi_{ii} = 2\delta + \sum_{j \in N} 2\delta + \left\| E_i^T P_i E_i \right\| \tag{30}$$

Selecting $\delta > 0$ to satisfy $\alpha_i > 0$ and the minimum eigenvalue of Q_i refers as $\lambda_{min}(Q_i)$, i is the the i-th subsystem.

Let combine the vectors as follows:

$$\begin{aligned} V_{vec}(x_i(k)) &:= [V_1(x_1(k)), V_2(x_2(k)), \ldots, V_N(x_N(k))]^T \\ \|x(k)\|_{vec} &:= \left[\|x_1(k)\|^2, \|x_2(k)\|^2, \ldots, \|x_N(k)\|^2 \right]^T \end{aligned}$$

$$\begin{aligned}\|e(k)\|_{vec} &:= \left[\|e_1(k)\|^2, \|e_2(k)\|^2, \ldots, \|e_N(k)\|^2\right]^T \\ \|f_i\|_{vec} &:= \left[\|f_1\|^2, \|f_2\|^2, \ldots, \|f_N\|^2\right]^T \\ \|C_i\|_{vec} &:= \left[\|C_1\|^2, \|C_2\|^2, \ldots, \|C_N\|^2\right]^T\end{aligned}$$

The inequality (23) could be compactly rewritten as:

$$\Delta V_i(x_i(k)) \leq A\|x(k)\|_{vec} + \Gamma\|e(k)\|_{vec} + \Psi\|f_i\|_{vec} \tag{31}$$

Assuming the spectral radius satisfies $r(A_{ii}^{-1}A_{ij}) < 1$ then,there is a $\mu > 0 \in \mathbb{R}_+^n$ such that $\mu^T A < 0$ [28]. The Lyapunov function selected as $V(x(k)) := \mu^T V_{vec}(x_i(k))$. Then ΔV yields:

$$\begin{aligned}\Delta V(x(k)) &= \mu^T \Delta V_{vec}(x_i(k)) \\ &\leq \mu^T A\|x(k)\|_{vec} + \mu^T\Gamma\|e(k)\|_{vec} \\ &\quad +\mu\Psi\|f_i\|_{vec}\end{aligned} \tag{32}$$

Assumption 4 *The demand load f_i directly affects the frequency of the power generation unit [29], which is represented by the output in our model $y = C_i x_i(k)$ as described in Section 2. So, for small f_i we assume that*

$$0 \leq \leq f_i \leq \epsilon\Delta\omega \leq \epsilon C_i X_i(k) \tag{33}$$

where ϵ is a positive or negative depending on the load's type if capacitive or inductive loads.

From (33) and (33) we can rewrite (33) as:

$$\Delta V(x(k)) \leq -L\|x(k)\|_{vec} + J\|e(k)\|_{vec} \tag{34}$$

where $L := \mu^T(A + \bar{\Psi})$ and $J := \mu^T\Gamma$ are row vectors.noticing that $\mu^T A < 0$ and $\bar{\Psi} := \epsilon C_i\Psi$.

Since,l_i and j_i are an entry of L and J vectors. So, we rewrite (34) as follows:

$$\begin{aligned}\Delta V(x(k)) &\leq \sum_{j\in N} l_i\|x_i(k)\|^2 + \sum_{j\in N} j_i\|e_i(k)\|^2 \\ &= -\sum_{j\in N}\left(l_i\|x_i(k)\|^2 - j_i\|e_i(k)\|^2\right)\end{aligned} \tag{35}$$

leading to asymptotic stability with $\sigma_i < \sqrt{\frac{l_i}{j_i}}$

4.3. Stability Analysis of a MAIPS subject to transmission delay

To achieve the asymptotic stability of the MAIPS in a normal situation with a round-robin protocol, we investigate selecting σ_i to deal with the error limits. However, MAIPS stability is not guaranteed if the system is experiencing transmission delays. Our aim in this part is to address the stability of MAIPS subject to transmission delay.

Theorem 3 *A multi-area interconnected power system (MAIPS) consists of N area as described in (1). The static feedback controller as in (6) is applied to control the frequency of MAIPS. Also, a sampling interval Δ satisfying Assumption 3. The MAIPS under the influence of the transmission delay with frequency and duration satisfying Assumption 2. this system is asymptotically stable if*

$$f_d + \Delta_* d_{max} < 1; \quad ,\omega_1 < 1 \tag{36}$$

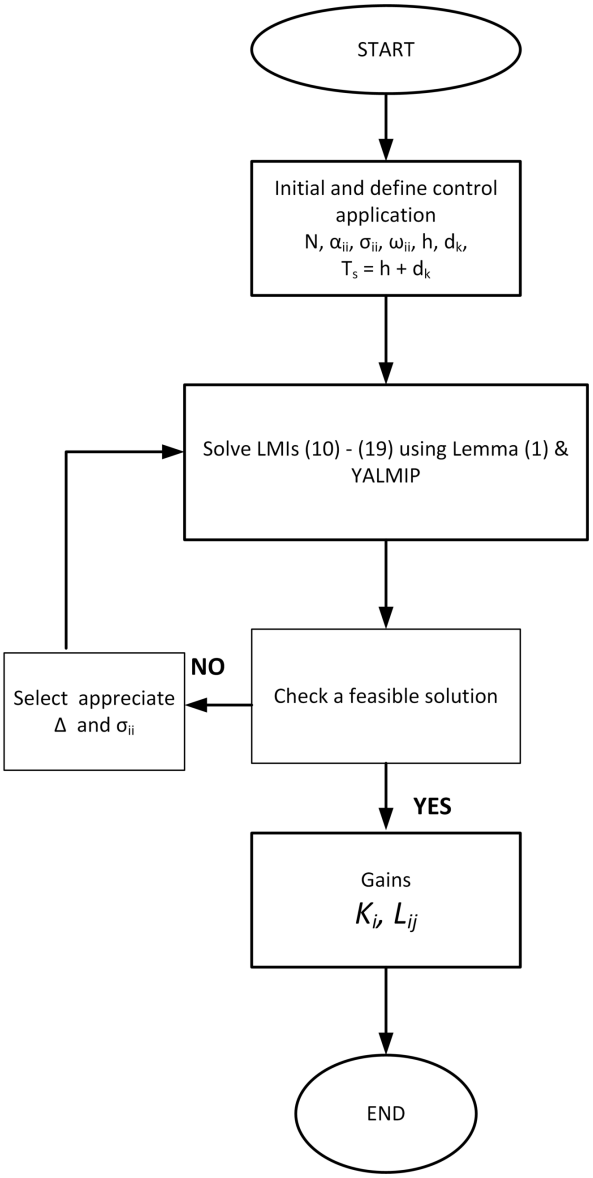

Fig. 2. Flowchart of the proposed static output feedback

where

$$\omega_1; = \min\left\{\frac{l_i - \sigma_i^2 j_i}{\lambda_{\max}(P_i)\mu_i}\right\}, \tag{37}$$

and $\Delta_* = N\Delta$, l_i, j_i, μ_i, *and* σ_i *are as in Lemma 1.*

Proof 4 *Theorem 3 proof is expressed in two main steps:*

1. *No delay periods. From Assumption 3, and (9) where* σ_i *satisfying Lemma 1 and (35)* < 0. *The*

Lyapunov function derivative is given as:

$$\begin{aligned}\Delta V(x(k)) &\leq -\sum_{j\in N}\left(l_i - j_i\sigma_i^2\right)\|x_i(k)\|^2 \\ &\leq -\sum_{j\in N}\frac{l_i - j_i\sigma_i^2}{\lambda_{max}(P_i)\mu_i}\mu_i V_i \\ &\triangleq -\omega_1 V(x(k))\end{aligned} \tag{38}$$

where $\omega_1 := \min\{\frac{l_i-\sigma_i^2 j_i}{\lambda_{\max}(P_i)\mu_i}\}$. *So, for* $k \in [h_n+\tau_n, T_{n+1}[$ *(no delay period), the Lyapunov function rewritten as:*

$$V(x(k)) \leq (1-\omega_1)^{k-h_n-\tau_n} V(x(h_n+\tau_n)) \tag{39}$$

2. *During delay. Introducing* z_m^i *as the last attempt successfully transmitted on the channel prior to the Trans. By considering* $e_i(k)$ *as mentioned previously, this leads to*

$$e_i(k) = x_i(z_m^i) - x_i(k) = x_i(h_n) - x_i(k) \tag{40}$$

and

$$\begin{aligned}\|e_i(k)\|^2 &\leq \|x_i(h_n)\|^2 + 2\|x_i(k)\|\,\|x_i(h_n)\| + \|x_i(k)\|^2 \\ &\leq 2\|x_i(h_n)\|^2 + 2\|x_i(k)\|^2\end{aligned} \tag{41}$$

for $k \in H_n$. *If* $\|e_i(k)\|^2$ *for* $i \in N$, *we will lead to*

$$\sum_{i\in N}\|e_i(k)\|^2 \leq 2\sum_{i\in N}\|x_i(h_n)\|^2 + 2\sum_{i\in N}\|x_i(k)\|^2 \tag{42}$$

If $\sum_{i\in N}\|x_i(h_n)\|^2 \leq \sum_{i\in N}\|x_i(k)\|^2$ *we have that* $\sum_{i\in N}\|e_i(k)\|^2 \leq 4\sum_{i\in N}\|x_i(k)\|^2$. *Otherwise, we have* $\sum_{i\in N}\|e_i(k)\|^2 \leq 4\sum_{i\in N}\|x_i(h_n)\|^2$

Calling (35), we can conclude that

$$\Delta V(x(k)) \leq \sum_{j\in N} j_i\|e_i(k)\|^2 \tag{43}$$

Thus, for all $k \in H_n$ *(transmission delay interval) If* $\sum_{i\in N}\|x_i(h_n)\|^2 \leq \sum_{i\in N}\|x_i(k)\|^2$, *the difference of the Lyapunov function rewritten as:*

$$\begin{aligned}\Delta V(x(k)) &\leq max\{j_i\}\sum_{j\in N}\|e_i(k)\|^2 \\ &\leq 4max\{j_i\}\sum_{j\in N}\|x_i(k)\|^2 \\ &\leq \frac{4max\{j_i\}}{min\{\mu_i\lambda_{min}(P_i)\}}\sum_{j\in N}\mu_i V(x_i(k)) \\ &\triangleq \omega_2 V(x(k))\end{aligned} \tag{44}$$

with $\omega_2 := \frac{4max\{j_i\}}{min\{\mu_i\lambda_{min}(P_i)\}}$. *Also,* $\forall k \in H_n$ *with* $\sum_{i\in N}\|x_i(h_n)\|^2 > \sum_{i\in N}\|x_i(k)\|^2$, *one has*

$$\Delta V(x(k)) \leq \omega_2 V(x(h_n)) \tag{45}$$

So, (44) and (45) implying that the Lyapunov function in the transmission delay period H_n satisfy the following equation

$$V(x(k)) \leq (1+\omega_2)^{k-h_n} V(x(h_n)) \tag{46}$$

During the transaction between stable and unstable modes.we will reflect the the protocol waiting time, the Lyapunov function in this instant $V(x(k)) \leq (1-\omega_1)^{k-h_n-\tau_n-N\Delta} V(x(h_n+\tau_n+N\Delta))$ for $t \in [h_n+\tau_n+N\Delta, T_{n+1}[$ and $V(x(k)) \leq (1+\omega_2)^{k-h_n} V(x(h_n))$ for $t \in [h_n, h_n+\tau_n+N\Delta[$.

In conclusion, the overall behavior of the closed-loop system could be treated as a switching system with two modes. So, when simple iterations are applied to the Lyapunov function in and out of the presence of the transmission delay status, we will get

$$V(x(k)) \leq (1-\omega_1)^{[k-\kappa_*-(f_d+\Delta_* d_{max})k]} (1+\omega_2)^{[\kappa_*+(f_d+\Delta_* d_{max})k]} V(x(0)) \tag{47}$$

To assure the stability of the last equation, (36) is obtained easily.

Remark 7 *Theorem 3 offers a criterion to characterize the stability of the distributed system in the form of (1) with an output feedback controller in the form of (6) and in the presence of transmission delay. The transmission delay is assumed to have constrained frequency and duration as described in Assumption 2. The signals are exchanged over a communication channel with sampling interval Δ satisfying Assumption 3.*

Remark 8 *The stability of the MAIPS is affected by the sampling interval (Δ) of the Round-robin protocol since it delimits when the overall system is able to repair communication. In the case where the bounded duration and frequency of the transmission delay subjected to the MAIPS with applying appropriate Round-robin inter-sampling time diminish the left-hand side of (36) that ensures the stability of the MAIPS. However, this is at the expense of high communication facilities.*

5. Simulation

The proposed static output control scheme is evaluated through a comprehensive simulation analysis, using a standard power system model Fig. 1 as a test case. A simulation result of three scenarios is shown in this section. The model incorporates various factors that affect the dynamics of the system, such as parameter changes, modeling errors due to disturbances in load and generation, time lag, and conventional generation sources. A MATLAB software version 2020a is used to construct a large-scale power system model with different tie-line dynamics to emulate a realistic system and test the performance of the proposed controller. The interconnected power system considered in (1) comprised of three subsystems are tested with parameters listed in Table 2. The controller gain calculated using YALMIP is given by

$$\begin{aligned} K_1 &= -1.376, K_2 = -2.433, K_3 = 0.852 \\ L_{12} &= -4.145, \quad L_{13} = -0.5034 \\ L_{21} &= -0.35, \quad L_{23} = -2.96 \\ L_{31} &= -0.671, \quad L_{32} = 0.482 \end{aligned} \tag{48}$$

A step load change of (0.1 p.u.) is applied in the three scenarios.

Figs. 3-6 show the simulation results for each case. The criteria for evaluating the performance are the frequency ($\Delta\omega$), the steady-state error, and the settling time.

Table 2. Areas parameters

Parameter	Area (1)	Area (2)	Area (3)
M_i^a	3.5	4.0	3.75
R_i^f	0.03	0.07	0.05
D_i	2	2.75	2.4
R_i	1	1	1
T_{CHi}	50	10	30
T_{G1}	40	25	32
B_i	1	1	1
T_{ij}	$T_{12} = T_{13} = 7.54$	$T_{21} = T_{23} = 7.54$	$T_{31} = T_{32} = 7.54$

5.1. Designed Controller in Nominal Situation

As can be seen from Fig. 3, the first states (frequencies) of the system in the three areas are restored to the acceptable ranges within 20 seconds under a nominal condition. Fig. 3 also demonstrates that the MAIPS is equilibrium under standard conditions with the controller gain given by (48). The controller applied can eliminate the frequency deviation whenever there is a load variation.

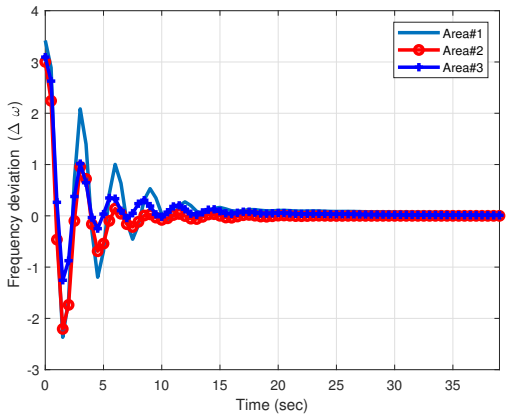

Fig. 3. The output of the system in the nominal situation with the designed controller

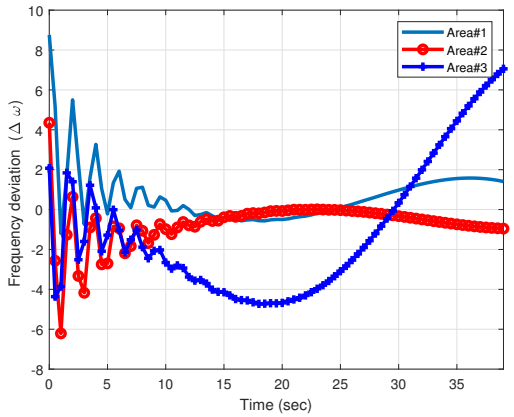

Fig. 4. The output of the system under transmission delay using the nominal T_s

5.2. Under Transmission Delay

In this scenario, a transmission delay was implemented on the system with the Assumption 2. In Fig. 4 the three interconnected power system is illustrated under the transmission delay characterized in section 3. The impact of a varying time delay of approximately $1-3$ seconds with a fixed sampling

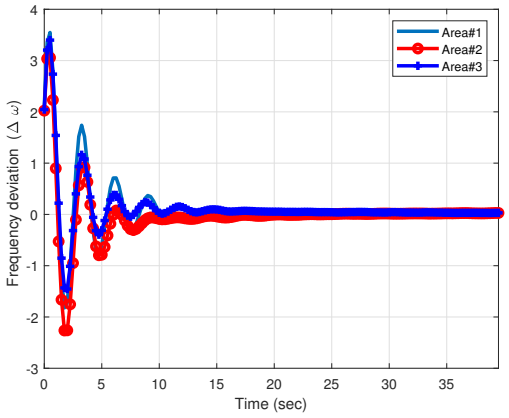

Fig. 5. The output of the system in the nominal situation using the modified T_s

time of $T_s = 0.1sec$ is illustrated in Fig. 4. As the time delay increases, the system frequency exhibits more oscillations and becomes unstable, failing to converge to its steady state value within the acceptable range. The maximum deviation of frequency is observed to be large.

5.3. Stabilization under Transmission Delay

Figs. 5 and 6 demonstrate that the system frequency of three interconnected areas can be stabilized by the proposed controller algorithm in the presence of time delay using a modified sampling interval of $T_s = 0.01sec$. The frequency deviation, overshoot, and settling time of the three interconnected power systems under nominal transmission conditions and two different sampling periods are presented in Figs. 3 and 5. The responses of the three areas in Fig. 5, have less overshoot and settle faster than those with the nominal sampling interval. Fig. 5 shows that the proposed design can achieve system performance to balance the load and generation with the adjusted sampling period.

Using Lemma 1 and YALMIP, we found the following:

$$P_1 = 10^{-6} \times \begin{bmatrix} 6.634 & 43.23 & -2.544 & 6049.83 \\ 24.22 & 2.756 & -23.245 & -4.761 \\ -5.674 & -14.275 & 4.79 & -84.784 \\ 549.80 & -4.51 & -12.73 & 8.004 \end{bmatrix}$$

$$P_2 = 10^{-6} \times \begin{bmatrix} 6.113 & 45.95 & -4.256 & 42.594 \\ 30.95 & 3.658 & -3.674 & -3.5485 \\ -2.668 & -20.674 & 1.8964 & -322.71 \\ 72.174 & -4.0481 & -263.71 & 8.976 \end{bmatrix},$$

$$P_3 = 10^{-6} \times \begin{bmatrix} 5.0538 & 2.467 & -2.035 & 60.134 \\ 62.462 & 2.5692 & -21.324 & -2.7112 \\ -2.063 & -20.618 & 2.5825 & -441.62 \\ 26.423 & -2.578 & -46.2 & 7.3178 \end{bmatrix},$$

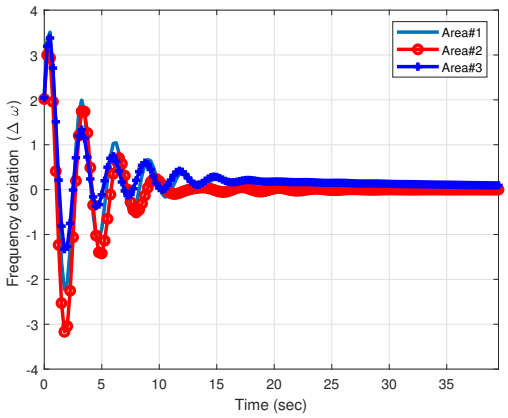

Fig. 6. The output of the system under transmission delay using the modified T_s

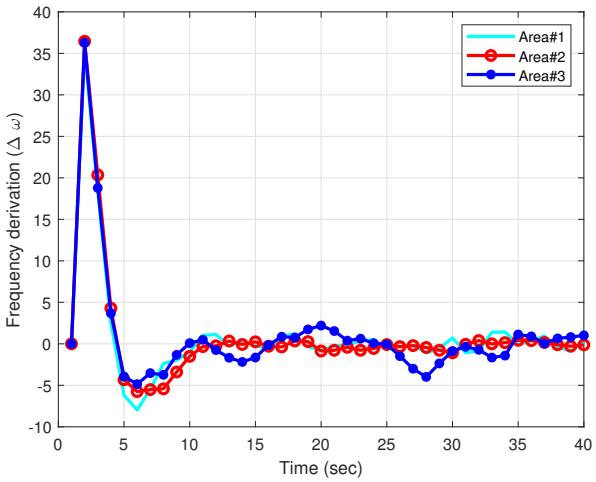

Fig. 7. The output of the system under transmission delay using the work in [30]

$$Q_1 = 10^{-7} \times \begin{bmatrix} 45.023 & 54.6235 & 5.257 & 5.1677 \\ 5.6775 & 7.3609 & 6.2751 & 5.7078 \\ 6.5657 & 2.2751 & 4.0092 & 5.8730 \\ 6.1737 & 4.7348 & 1.0630 & 6.5553 \end{bmatrix},$$

$$Q_2 = 10^{-5} \times \begin{bmatrix} 45.2651 & 6.7758 & 20.8955 & 9.1632 \\ 4.0258 & 6.1497 & 8.1212 & 2.011 \\ 3.5455 & 7.1612 & 6.2509 & 5.7868 \\ 5.1653 & 2.7691 & 14.3668 & 1.8793 \end{bmatrix},$$

$$Q_3 = 10^{-5} \times \begin{bmatrix} 45.918 & 3.6566 & 5.1118 & 6.1551 \\ 5.7346 & 7.4899 & 6.2784 & 7.2669 \\ 0.2918 & 3.2184 & 5.2896 & 9.7211 \\ 2.1556 & 3.2376 & 3.7213 & 3.4172 \end{bmatrix}$$

Then we obtain:

$$A = 10^{-6} \times \begin{bmatrix} 0.402 & 0.546 & 0.235 \\ 0.084 & 0.384 & 0.348 \\ 0.170 & 0.097 & 0.656 \end{bmatrix}$$

$$\Gamma = 10^{-6} \times \begin{bmatrix} 0.481 & 0.284 & 0.355 \\ 0.366 & 0.766 & 0.144 \\ 0.367 & 0.902 & 0.886 \end{bmatrix},$$

$$\Psi = 10^{-8} \times \begin{bmatrix} 0.654 & 0 & 0 \\ 0 & 0.557 & 0 \\ 0 & 0 & 0.364 \end{bmatrix}$$

Since the σ_1, σ_2 and σ_3 are (0.869), (1.002), and (0.972), respectively. the σ, in this case, is chosen to be (0.8). Based on Assumption 3, we select the sampling interval $\Delta = 0.25$s. From this we calculate ω_1,ω_2 and ω_3 to be $(3.004(10)^4)$,and (1.458), respectively. As shown in Figs. 6, the designing parameters are able to maintain the stability of the MAIPS in the presence of the DoS attack and stable the frequency to the nominal state. The DoS attack was modeled based on Theorem 3 The stability of the system under the DoS attack was ensured by the proposed controller, as demonstrated in Figs. 5 and 6. By comparing the proposed method of static output feedback with a modified sampling interval with another method [30] in Fig. 7 under time delay and load variations, the effectiveness of the proposed method is shown. By tuning the sampling period of the Robin communication protocol, the frequency deviation in the proposed method has a faster settling time and less overshoot than the method in Fig. 7.

6. Conclusion

This study examines novel output feedback for a cyber-physical system that includes power networks. It analyzes the stability of a round-robin communication system when faced with mixed cyberattacks and load variations. A static feedback controller with an adjusted sampling time is designed to maintain the stability of a multi-area interconnected power system (MAIPS) while minimizing the required performance function. The stability of the MAIPS is then determined when it is subjected to transmission delays, taking into account pre-established parameters for the delay's duration and frequency. Our findings indicate that time delays can influence system stability and that choosing an appropriate sampling interval is necessary to ensure the desired stability of the system. The proposed approach's feasibility is demonstrated through an example involving three interconnected power network areas under various scenarios.

Based on the conclusion of this study, here are some additional future suggestions and directions for research:

- Investigating the impact of multiple cyberattacks and unknown loads: The study focused on mixed cyberattacks and load variations, but did not consider the effects of multiple cyberattacks or unknown loads on system stability. Future research could explore the stability of the system under multiple simultaneous cyberattacks and how unknown loads affect system performance.
- Dynamic event-triggered output feedback: The study used a static feedback controller with an adjusted sampling time, but dynamic event-triggered output feedback may be a more effective approach for maintaining stability. Future research could investigate the use of dynamic event-triggered output feedback and compare its performance to that of the static feedback controller used in this study.
- Fault isolation in networked cyber-physical systems: The study did not examine the problem of fault isolation in networked cyber-physical systems. Future research could investigate fault

isolation techniques that can detect and isolate faults in the system, ensuring that any failures do not propagate and lead to system instability.

- Developing real-time monitoring and control techniques: As power networks become more complex and interconnected, real-time monitoring and control become increasingly important for maintaining stability. Future research could explore the development of advanced monitoring and control techniques that can detect and respond to changes in the system in real time.
- Incorporating renewable energy sources: The study did not specifically consider the impact of renewable energy sources on system stability. Future research could examine how renewable energy sources, such as solar or wind power, affect system stability and explore ways to optimize the integration of renewable energy sources into the power network.

References

[1] J. Alipoor, Y. Miura, and T. Ise, "Power system stabilization using virtual synchronous generator with alternating moment of inertia," *IEEE Journal of Emerging and Selected Topics in Power Electronics*, vol. 3, no. 2, pp. 451–458, 2014, https://doi.org/10.1109/JESTPE.2014.2362530.

[2] L. M. Castro and E. Acha, "On the provision of frequency regulation in low inertia ac grids using hvdc systems," *IEEE Transactions on Smart Grid*, vol. 7, no. 6, pp. 2680–2690, 2015, https://doi.org/10.1109/TSG.2015.2495243.

[3] W. Zhang, K. Rouzbehi, A. Luna, G. B. Gharehpetian, and P. Rodriguez, "Multi-terminal hvdc grids with inertia mimicry capability," *IET Renewable Power Generation*, vol. 10, no. 6, pp. 752–760, 2016, https://doi.org/10.1049/iet-rpg.2015.0463.

[4] C. N. S. Kalyan and C. V. Suresh, "Higher order degree of freedom controller for load frequency control of multi area interconnected power system with time delays," *Global Transitions Proceedings*, vol. 3, no. 1, pp. 332–337, 2022, https://doi.org/10.1016/j.gltp.2022.03.020.

[5] S. Sridhar, A. Hahn, and M. Govindarasu, "Cyber–physical system security for the electric power grid," *Proceedings of the IEEE*, vol. 100, no. 1, pp. 210–224, 2011, https://doi.org/10.1109/JPROC.2011.2165269.

[6] M. Vrakopoulou, P. M. Esfahani, K. Margellos, J. Lygeros, and G. Andersson, "Cyber-attacks in the automatic generation control," in *Cyber Physical Systems Approach to Smart Electric Power Grid*, 2015, pp. 303–328, https://doi.org/10.1007/978-3-662-45928-7_11.

[7] D. Ding, Q.-L. Han, Y. Xiang, X. Ge, and X.-M. Zhang, "A survey on security control and attack detection for industrial cyber-physical systems," *Neurocomputing*, vol. 275, pp. 1674–1683, 2018, https://doi.org/10.1016/j.neucom.2017.10.009.

[8] M. Khalaf, A. Youssef, and E. El-Saadany, "Joint detection and mitigation of false data injection attacks in agc systems," *IEEE Transactions on Smart Grid*, vol. 10, no. 5, pp. 4985–4995, 2018, https://doi.org/10.1109/TSG.2018.2872120.

[9] Y. Zhang and T. Yang, "Decentralized switching control strategy for load frequency control in multi-area power systems with time delay and packet losses," *IEEE Access*, vol. 8, pp. 15 838–15 850, 2020, https://doi.org/10.1109/ACCESS.2020.2967455.

[10] K. Yan, X. Liu, Y. Lu, and F. Qin, "A cyber-physical power system risk assessment model against cyberattacks," *IEEE Systems Journal*, vol. 17, no. 2, pp. 2018–2028, 2023, https://doi.org/10.1109/JSYST.2022.3215591.

[11] K. Pan, P. Palensky, and P. M. Esfahani, "From static to dynamic anomaly detection with application to power system cyber security," *IEEE Transactions on Power Systems*, vol. 35, no. 2, pp. 1584–1596, 2019, https://doi.org/10.1109/TPWRS.2019.2943304.

[12] C.-W. Ten, C.-C. Liu, and G. Manimaran, "Vulnerability assessment of cybersecurity for scada systems," *IEEE Transactions on Power Systems*, vol. 23, no. 4, pp. 1836–1846, 2008, https://doi.org/10.1109/TPWRS.2008.2002298.

[13] M. S. Mahmoud, M. M. Hamdan, and U. A. Baroudi, "Modeling and control of cyber-physical systems subject to cyber attacks: A survey of recent advances and challenges," *Neurocomputing*, vol. 338, pp. 101–115, 2019, https://doi.org/10.1016/j.neucom.2019.01.099.

[14] M. S. Mahmoud and Y. Xia, *Cloud Control Systems: Analysis, Design and Estimation*. Academic Press, 2020, https://books.google.co.id/books?id=w2_KDwAAQBAJ.

[15] A. Gundes and L. Kabuli, "Load frequency control of multi-area interconnected power systems with time delays," *IEEE Transactions on Control of Network Systems*, 2021, https://doi.org/10.1109/TCNS.2021.3122523.

[16] B. S. S. Rithigaa, K. Vamshi, A. Jawahar, and K. Ramakrishnan, "Lyapunov stability analysis of load frequency control systems with communication network induced time-delays and ev aggregator," in *2021 9th IEEE International Conference on Power Systems (ICPS)*, 2021, pp. 1–6, https://doi.org/10.1109/ICPS52420.2021.9670015.

[17] A. Dev, V. Léchappé, and M. K. Sarkar, "Prediction-based super twisting sliding mode load frequency control for multi-area interconnected power systems with state and input time delays using disturbance observer," *International Journal of Control*, vol. 94, no. 7, pp. 1751–1764, 2021, https://doi.org/10.1080/00207179.2019.1673487.

[18] A. Jawahar and K. Ramakrishnan, "Further improvement in stability and stabilization margin of micro-grid load frequency control system with constant communication delays," in *Proceedings of Symposium on Power Electronic and Renewable Energy Systems Control*, 2021, pp. 185–194, https://doi.org/10.1007/978-981-16-1978-6_16.

[19] H. H. Alhelou, N. Nagpal, N. Kassarwani, and P. Siano, "Decentralized optimized integral sliding mode-based load frequency control for interconnected multi-area power systems," *IEEE Access*, 2023, https://doi.org/10.1109/ACCESS.2023.3262790.

[20] M. S. Mahmoud and Y. Xia, *Networked control systems: cloud control and secure control*. Butterworth-Heinemann, 2019, https://doi.org/10.1016/B978-0-12-816119-7.00012-5.

[21] Z. Song, Y. Liu, and M. Tan, "Robust pinning synchronization of complex cyberphysical networks under mixed attack strategies," *International Journal of Robust and Nonlinear Control*, vol. 29, no. 5, pp. 1265–1278, 2019, https://doi.org/10.1002/rnc.4436.

[22] C.-H. Xie and G.-H. Yang, "Observer-based attack-resilient control for linear systems against fdi attacks on communication links from controller to actuators," *International Journal of Robust and Nonlinear Control*, vol. 28, no. 15, pp. 4382–4403, 2018, https://doi.org/10.1002/rnc.4236.

[23] H. Bevrani, *Robust power system frequency control*. Springer, 2014, https://doi.org/10.1007/978-3-319-07278-4.

[24] S. Feng, P. Tesi, and C. De Persis, "Towards stabilization of distributed systems under denial-of-service," in *2017 IEEE 56th Annual Conference on Decision and Control (CDC)*, 2017, pp. 5360–5365, https://doi.org/10.1109/CDC.2017.8264453.

[25] C. De Persis, R. Sailer, and F. Wirth, "On inter-sampling times for event-triggered large-scale linear systems," in *52nd IEEE Conference on Decision and Control*, 2013, pp. 5301–5306, https://doi.org/10.1109/CDC.2013.6760723.

[26] M. Mazo and P. Tabuada, "Decentralized event-triggered control over wireless sensor/actuator networks," *IEEE Transactions on Automatic Control*, vol. 56, no. 10, pp. 2456–2461, 2011, https://doi.org/10.1109/TAC.2011.2164036.

[27] M. S. Mahmoud and H. N. Nounou, "Simultaneous output feedback stabilization of time-delay systems," *IMA Journal of Mathematical Control and Information*, vol. 23, no. 2, pp. 211–223, 2006, https://doi.org/10.1093/imamci/dni054.

[28] S. Dashkovskiy, H. Ito, and F. Wirth, "On a small gain theorem for iss networks in dissipative lyapunov form," *European Journal of Control*, vol. 17, no. 4, pp. 357–365, 2011, https://doi.org/10.3166/ejc.17.357-365.

[29] A. Molina-García, I. Munoz-Benavente, A. D. Hansen, and E. Gomez-Lazaro, "Demand-side contribution to primary frequency control with wind farm auxiliary control," *IEEE transactions on power systems*, vol. 29, no. 5, pp. 2391–2399, 2014, https://doi.org/10.1109/TPWRS.2014.2300182.

[30] N. M. Alyazidi and M. S. Mahmoud, "On lqg control design for network systems with/without acknowledgments using a particle filtering technology," *Applied Mathematics and Computation*, vol. 359, pp. 52–70, 2019, https://doi.org/10.1016/j.amc.2019.04.012.